Double-layered TiO$_2$/activated carbon films with enhanced photocatalytic activity towards methylene blue degradation

PORNSIT LORKIT[a,b], NUNTANID PHATHARAPEETRANUN[a], BUSSARIN KSAPABUTR[a,b,*],
SUJITRA WONGKASEMJIT[c], NATTAWUT CHAIYUT[a], MANOP PANAPOY[a,b,*]

[a]*Department of Materials Science and Engineering, Faculty of Engineering and Industrial Technology,
Silpakorn University, Sanamchandra Palace Campus, Nakhon Pathom 73000, Thailand*
[b]*High Performance and Smart Materials, Center of Excellence for Petrochemical and Materials Technology,
Chulalongkorn University, Bangkok 10330, Thailand*
[c]*The Petroleum and Petrochemical College, Chulalongkorn University, Bangkok 10330, Thailand*

Double-layered films of TiO$_2$ and activated carbon were fabricated on aluminum substrates by electrophoretic deposition. Moreover, TiO$_2$ powder was synthesized by solvothermal process. The photocatalytic efficiency and reusability of the resulting films were tested for the photodegradation of methylene blue under ultraviolet irradiation. The double-layered films obtained using the synthesized TiO$_2$ exhibited the highest photodegradation efficiency (94%) for removing methylene blue. The immobilized film could solve the problem of separation and recovery of powder catalyst in practical applications. Therefore, the imobilized systems are an advantage for wastewater treatment because they are cost-effective, eco-friendly and reusable with relatively high photocatalytic performance.

1. Introduction

Photocatalytic degradation has attracted much more attention because of its high potential to promote the removal of organic pollutants in wastewater. Titanium dioxide (TiO$_2$) has been extensively studied as a promising material for environment protection over the past few decades. TiO$_2$ is a semiconductor photocatalyst, which is biologically inert, photoactive, non-toxic, inexpensive and biocompatible, and is able to be widely used for treatment of wastewater by photocatalytic process and very efficient under ultraviolet light irradiation [1–3]. Most studies have focused on the development and performance of TiO$_2$. Some attempts have been made to prepare TiO$_2$ nanoparticles on some supports such as carbon nanotube [4–5], ceramic [6–7], and activated carbon [8–9] for the photocatalytic degradation of toxic pollutants. Among several types of support materials, activated carbon (AC) is the most attractive one because of its high surface area, offering concentrated organic pollutant near TiO$_2$ surface by adsorption [10–11] and in contact with TiO$_2$, and its reduction in the recombination of photogenerated electron–hole [12]. El-Salamony et al. [10] prepared TiO$_2$/AC nanocomposite powders through a mechano-mixing method and found that the supporting of TiO$_2$ on AC powders produced catalysts with higher surface area and photoactivity than pure TiO$_2$. Xing et al. [13] prepared photocatalysts comprising nanosized TiO$_2$ particles on

activated carbon powders by a sol-gel method for the removal of Rhodamine B from water. Tamilselvi et al. [14] synthesized an activated carbon fiber from silk cotton fiber and then was converted into a photocatalyst by loading nano-TiO$_2$ powder. It has shown effectiveness in the removal of organic pollutants from industrial wastewater and effluents. However, one of critical problems still hindering further large scale application of the TiO$_2$/AC composite powders in wastewater treatment is the lack of reproducibility and the difficulty in the separation of powder from water after the photocatalytic degradation process [15–16]. The fabrication of TiO$_2$/AC composite in the form of thin film has been targeted to solve the problems. Nevertheless, the difference in photocatalytic efficiency can be attributed to the surface area of thin film being smaller than the surface area of powder and the mass transfer limitation of organic pollutant to the surface of TiO$_2$ [16]. Therefore, the immobilization of TiO$_2$ in the form of a thin film on high surface area support has emerged as an alternative water treatment method for improving the photocatalytic performance. Electrophoretic deposition (EPD) is a practical method for colloidal material processing which is gaining increasing interest as a rapid, simple and versatile technique for the production of coatings and films from nanoparticles and carbon materials [17–18].

In the present work, we are planning to report TiO$_2$/AC double-layered films as a photocatalyst by the

coating of TiO_2 particles onto the surface of AC film fabricated using EPD technique with no use of binder, which showed a promising photocatalytic activity than pure TiO_2 due to the synergistic effect between AC supporting materials and TiO_2 layer. The efficiency and reusability of the TiO_2/AC double-layered films were quantified by degrading methylene blue (MB) under UV light in comparison with single-layered films from commercially available standard TiO_2 (P25), synthesized TiO_2 and AC and double-layered film of P25/AC prepared by EPD process, which is of fundamental importance for an economical and eco-friendly scaling-up of such systems.

2. Experimental

2.1. Preparation of catalyst

An electrophoretic deposition system was used to deposit the TiO_2/AC (AC; Karbokarn Co., Ltd., BET surface area of about 816.65 m^2/g, pore volume of 0.4642 mL/g and mean pore diameter of 2.274 nm) and TiO_2 films. The electrophoretic cell contained two electrodes (anode and cathode) made of stainless steel plate. An aluminum foil substrate was located at the cathode. The applied voltage, distance between two electrodes and deposition time of each layer were controlled at 50 V, 2 cm and 15 min, respectively at room temperature.

Firstly, TiO_2 powder was synthesized by solvothermal process at 200 °C for 72 h using a starting solution of titanium tetraisopropoxide (TTIP; Acros Organics, >98%), distilled water, and isopropyl alcohol (Carlo Erbra Reagents, >99.7%) at a volume ratio of 1 : 2 : 33. Then, it was calcined at 600 °C for 2 h in an ambient atmosphere. This sample was designated as STC6.

The STC6/AC and P25/AC double-layered films were fabricated by firstly depositing AC on the aluminum foil substrate followed by TiO_2 coating using EPD process. Meanwhile single-layered films of AC, STC6 and commercially available standard TiO_2 (P25) were deposited directly on the aluminum foil substrate for comparison.

2.2. Characterization

The crystal structure and morphology of the prepared TiO_2 and P25 powders were characterized by X-ray diffraction (XRD; Bruker D8) using Cu$K\alpha$ radiation at a wavelength of 0.1514 nm and transmission electron microscopy (TEM; JEOL 2100), respectively. Brunauer–Emmett–Teller (BET) method (Quantachrome, Autosorb–1) was used to obtain the specific surface area of the synthesized TiO_2 and commercial P25 powders.

After film deposition, the surface morphology was examined using a scanning electron microscope (SEM; Hitachi S3400N). Also, the methylene blue (MB, Carlo Erba Reagents) adsorption method was used to obtain the specific surface area of the fabricated films. The

photocatalytic efficiency of the prepared films for the degradation of MB was evaluated under UV light irradiation (Philips, Hg-Lamp 400W) at light intensity of 5.1 mW/cm^2. The efficiency of MB removal was calculated by the following equation:

$$\eta = 100(C_0 - C)/C_0 \qquad (1)$$

where C_0 and C represent the initial concentration of MB before irradiation and the concentration of MB after irradiation for a given time, respectively.

3. Results and discussion

The XRD patterns of commercial TiO_2 (P25) and synthesized TiO_2 (STC6) powders are shown in Fig. 1. The commercial P25 powder is composed of a mixture of anatase and rutile phases, while the STC6 powder contains only anatase phase. The phase composition of both samples is present in Table 1. The characteristic peaks of anatase and rutile phases can be identified which are consistent with JCPDS File no. 00–021–1272 and 00–021–1276, respectively. The average crystallite sizes of P25 and SCT6 samples were calculated using Scherrer′s formula [19] from the diffraction peak at 25.28 and 27.45° for anatase and rutile phases, respectively and reported in Table 1.

Table 1. Phase content, crystallite size and S_{BET} of STC6 and P25 powders

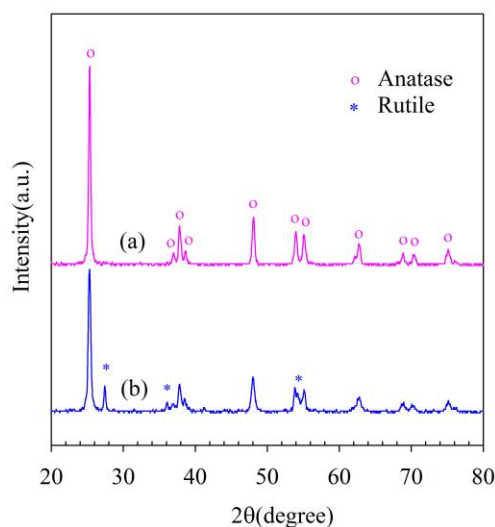| Sample	STC6	P25	
	Anatase	Anatase	Rutile
Phase content (%)	100	75	25
Crystallite size (nm)	29.13	20.00	23.87
S_{BET} (m^2g^{-1})	31.74	48.47	

Fig. 1. XRD patterns of (a) STC6 and (b) P25 powders

Fig. 2 presents the TEM images of P25 and STC6 powders. It can be observed that the particle size of STC6 was larger than that of P25, which was in good agreement with the XRD results. Additionally, the specific surface area (S$_{BET}$) of P25 and STC6 powders measured by BET is shown in Table 1. The specific surface area of STC6 powder was slightly lower than that of P25. This might be because the particles with smaller sizes had larger surface areas. These results were consistent with those reported by Li et al. [20].
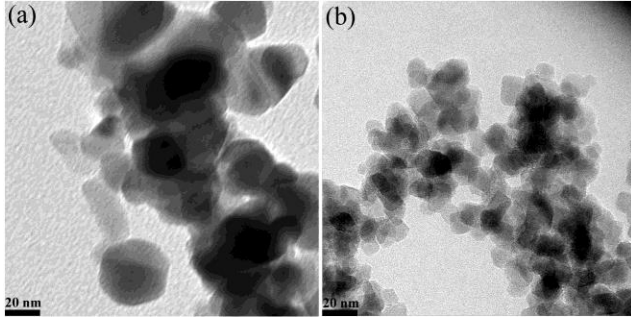

Fig. 2. TEM micrographs of (a) STC6 and (b) P25 powders

The surface morphology of single-layered films of P25 and STC6 after deposition on aluminum substrate is displayed in Fig. 3 (a)–(b). Both the TiO$_2$ films showed porous morphology. However, the STC6 film had a looser packing of particles and therefore higher porosity. Meanwhile the P25 film showed a better packing of particles leading to a denser coating with crack formation because smaller particles move much more quickly and easily than larger ones at the same electric field [21]. For the double-layered films of different TiO$_2$ particles on AC layer deposited on the aluminum substrate (Fig. 3(c)–(d)), it was found that P25 particles could completely cover the AC layer whereas STC6 particles did not completely cover the AC layer. Grinis et al. [22] reported that suspension stability affected the deposition efficiency for EPD technique. Because of its larger particle size, TiO$_2$ particles tend to be more unstable, resulting in a rough surface. Chang et al. [23] added magnesium nitrate hexahydrate (Mg(NO$_3$)$_2$.6H$_2$O) in electrolyte solution to improve the stability of TiO$_2$ particles and help to minimize the formation of cracks. However, this study indicated that the uniform and porous films could be prepared without added additives.
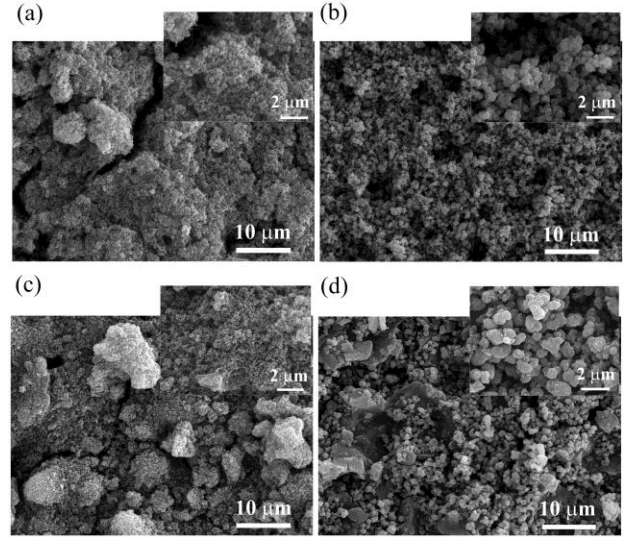

Fig. 3. SEM images of (a) P25 film, (b) STC6 film, (c) AC/P25 film, and (d) AC/STC6 film (the insets show the corresponding magnified SEM images)

Fig. 4 shows the adsorption of MB in the equilibrium for single-layered and double-layered films. In all the films, the amount of solute adsorbed per unit weight of adsorbent at equilibrium (Q_e (mg/g)) is a function of concentration in the liquid phase at equilibrium (C_e (mg/l)). The specific surface area can be calculated from the following relation [24]:

$$S_{MB} = (q_m \times A_{MB} \times N_A)/(M \times 1000) \qquad (2)$$

where S_{MB} is the specific surface area (m^2/g), N_A is Avogadro's number (6.02 × 10^{23} mol^{-1}), A_{MB} is the occupied surface area of one molecule of MB (197.2 Å^2), M is the molecular weight of MB (319.89 g/mol) and q_m is the number of molecules of MB adsorbed at the monolayer (mg/g), which is calculated from the Langmuir model. An empirical model was represented as follows [25]:

$$Q_e = (q_m K C_e)/(1 + K C_e) \qquad (3)$$

where Q_e (mg/g) is the amount of solute adsorbed per unit weight of adsorbent at equilibrium, C_e (mg/L) is the concentration in the liquid phase at equilibrium, q_m (mg/g) is the theoretical maximum adsorption capacity and K (L/mg) is the Langmuir adsorption constant.
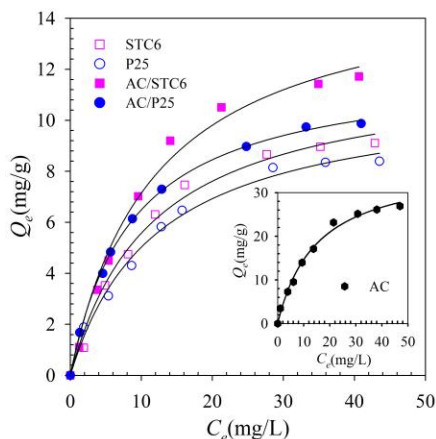
Fig. 4. Langmuir adsorption isotherm fitted to the experimental data for adsorption of MB onto different films

The MB adsorption method indicated that AC film exhibited the highest specific surface area. This trend was related with the result of BET surface area of AC powder. The specific surface area obtained by MB adsorption measurement of STC6 film was higher than that of P25 film, which was opposite to the results obtained from BET measurement because of more loosely packed particles and higher porosity of STC6 film. The coating of TiO_2 powders on AC layer leads to an increase in the specific surface area of double-layered films, as seen in Table 2. The STC6/AC film showed higher specific surface area than the P25/AC film, probably owing to incomplete coverage of STC6 on the AC layer.

Table 2. Langmuir parameter and specific surface area of various films

Sample	Langmuir parameter			S_{MB} (m^2/g)
	q_m (mg/g)	K (L/mg)	R^2	
P25	11.14	0.082	0.992	27.27
STC6	12.01	0.087	0.991	29.40
P25/AC	12.13	0.115	0.999	29.69
STC6/AC	15.63	0.084	0.991	38.26
AC	36.62	0.067	0.993	89.63

To investigate the photocatalytic efficiency of the film photocatalyst, the degradation of MB used as a model dye pollutant was tested under UV irradiation, as presented in Fig. 5(a). It was observed that STC6/AC double-layered film exhibited the maximum MB removal efficiency of 93.37% at 60 min. Because STC6/AC double-layered film with high specific surface area can adsorb MB by providing more available sites for binding MB and thereby improving sorption–degradation [17]. The kinetics of MB degradation profiles are illustrated in Fig. 5(b). The photocatalytic degradation of MB fitted pseudo-first-order kinetics expressed as:

$$-dC/dt = k_{app}C \qquad (4)$$

Integrating this equation (with the restriction $C = C_0$ at $t = 0$, with C_0 being the initial concentration and t is the reaction time) gives the following relation [26]:

$$\ln(C_o/C) = k_{app}t \qquad (5)$$

where C is the reactant concentration at a given time. The apparent rate constant (k_{app}) of the photocatalytic reaction and the removal efficiency (η) are reported in Table 3. The STC6/AC double-layered film provided the highest value of k_{app} and η due to its high specific surface area.

Table 3. The photocatalytic parameters of MB removal by different films

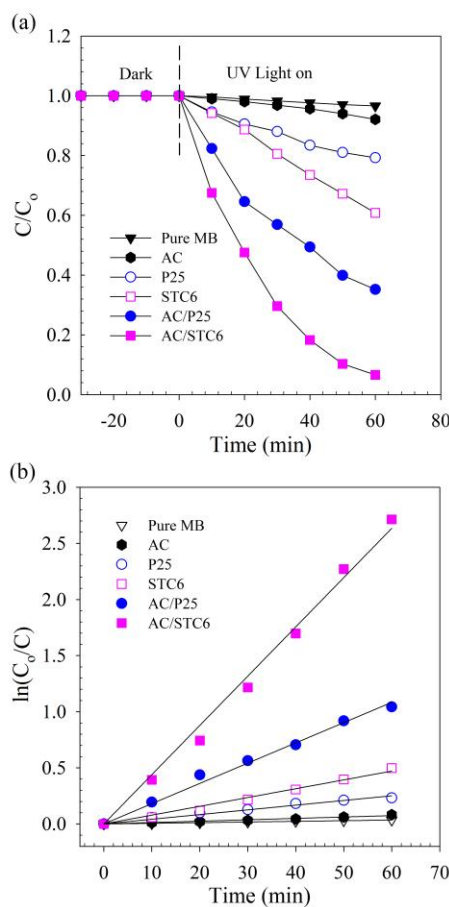| Sample	R^2	k_{app} (min^{-1})	η at 60 min (%)
AC	0.972	0.001	7.89
P25	0.977	0.004	20.79
STC6	0.985	0.008	39.20
AC/P25	0.990	0.018	64.78
AC/STC6	0.992	0.044	93.37

Fig. 5. (a) Variation of MB concentration as a function of irradiation time (with the time of light on set as 0) and (b) degradation kinetics of MB over different film catalysts

The photocatalytic degradation of MB for the STC6/AC film followed the Langmuir–Hinshelwood model, which is mostly used to explain the heterogeneous photocatalysis, as follows [27]:

$$-dC/dt = k_{app}C = kKC/(1 + KC_o) \qquad (6)$$

$$1/k_{app} = 1/kK + C_o/k \qquad (7)$$

where k is the reaction rate constant and K is the adsorption equilibrium constant.

The rate constant of surface reaction (k) and the adsorption equilibrium constant (K) can be obtained from the slope and intercept in the plot of $1/k_{app}$ versus C_0, respectively. In Fig. 6, the calculated k and K values were 1.210 mg/(L·min) and 0.079 L/mg, respectively. The correlation coefficient (R^2) of the linear plot was 0.99, indicating that the MB photodegradation catalyzed using STC6/AC film fitted the Langmuir-Hinshelwood kinetic model.

The reusability of the photocatalysts is one of crucial factors for their practical application to make the process free of waste and also reduce the operational cost. To investigate the photocatalyst reusability, the STC6/AC double-layered film was easily recovered from the reaction mixture without filtration. The recovered catalyst was then reused for the photodegradation of MB under the same reaction condition as described above. The reusability of STC6/AC double-layered film was tested for five cycles (Fig. 7). After being reused for five times, the STC6/AC catalyst film still preserved its photocatalytic efficiency for MB degradation. This reusability of STC6/AC film is attributed to the stability and resistance to photocorrosion. Therefore, it can be used as an efficient photocatalyst for the degradation of MB.
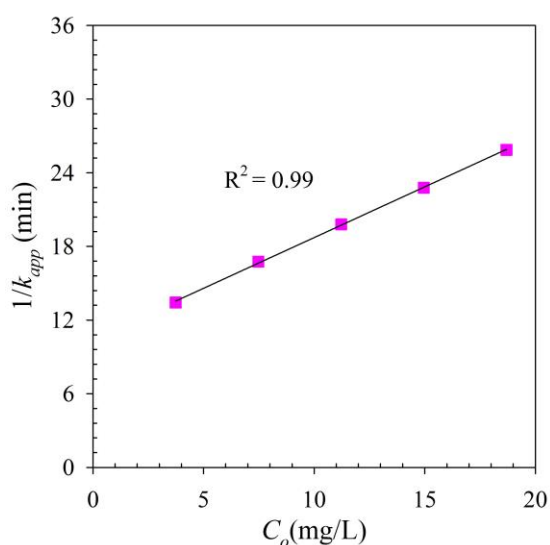

Fig. 7. Reusability of the STC6/AC film for five cycles

4. Conclusions

The TiO₂/activated carbon double-layered film photocatalyts were prepared using an electrophoretic deposition technique with no added additives. Moreover, TiO₂ powder was synthesized through a solvothermal method. The photocatalytic efficiency of methylene blue degradation for TiO₂/activated carbon films was studied using methylene blue as a model pollutant. The synthesized TiO₂/activated carbon films showed higher photocatalytic performance than the commercial TiO₂/activated carbon film and their single-layered films owing to more available sites for binding MB molecules. Moreover, a reusability study also presented that the double-layered film of the synthesized TiO₂/activated carbon with high photocatalytic efficiency and stability could be a promising candidate for its practical application in environmental issues.

Fig. 6. The relationship between the $1/k_{app}$ versus the initial concentration of MB. Experimental conditions: temperature of 25 ºC and reaction time of 60 min
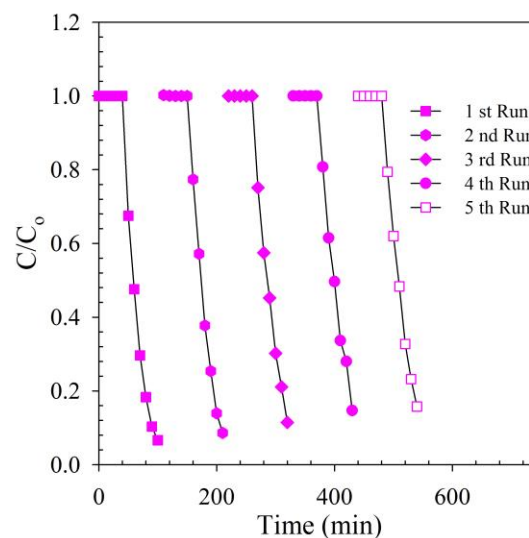
References

[1] H. U. Lee, S. C. Lee, J. Won, B.-C. Son, S. Choi, Y.

Kim, S. Y. Park, H.-S. Kim, Y.-C. Lee, J. Lee, Sci. Rep. **5**, 8691 (2015).

[2] H.Yao, M. Fan, Y. Wang, G. Luo, W. Fei, J. Mater. Chem. A. **3**, 17511 (2015).

[3] N. Sangkharat, N. Chaiyut, B. Ksapabutr, M. Panapoy, Ceram. Int. **42**, 5858 (2016).

[4] M. M. Mohamed, RSC Adv. **5**, 46405 (2015).

[5] A. A. Ashkarran, M. Fakhari, H. Hamidinezhad, H. Haddadi, M. R. Nourani, J. Mater. Res. Technol. **4**(2), 126 (2015).

[6] W. M. Liu, Chem. Res. Chin. Univ. **29**, 314 (2013).

[7] S. Izadyar, S. Fatemi, Ind. Eng. Chem. Res. **52**(32), 10961 (2013).

[8] C. P. Sajan, S. Wageh, A. A. Al-Ghamdi, J. Yu, S. Cao, Nano. Res. **9**, 3 (2016).

[9] D. Chen, L. Zou, S. Li, F. Zheng, Sci. Rep. **6**, 20335 (2016).

[10] R. A. El-Salamony, E. Amdeha, S. A. Ghoneim, N. A. Badawy, K. M. Salem, A. M. Al-Sabagh, Environ. Technol. **1** (2017).

[11] L. Zhu, J.-H. Cho, Z.-D. Meng, J.-G. Choi, C.-Y. Park, T. Ghosh, W.-C. Oh, Asian J. Chem. **25**, 688 (2013).

[12] P. S. Yep, T. T. Lim, M. Lim, M. Srinivasan, Catal. Today. **151**, 8 (2010).

[13] B. Xing, C. Shi, C. Zhang, G. Yi, L. Chen, H. Guo, G. Huang, J. Cao, J. Nanomater. **2016**, 10 (2016).

[14] S. Tamilselvi, M. Asaithambi, P. Sivakumar, Desalin. Water Treat. **57**, 15495 (2016).

[15] B. Ksapabutr, W. Thong-Oun, M. Panapoy, Funct. Mater. Lett. **2**, 179 (2009).

[16] H. Dong, G. Zeng, L. Tang, C. Fan, C. Zhang, X. He, Y. He, Water Res. **79**, 128 (2015).

[17] X. Zhang, L. Lei, J. Hazard. Mater. **153**, 827 (2008).

[18] A. A. Dougna, B. Gombert, T. Kodom, G. D.-Boundjou, S. O. B. Boukari, N. K. V. Leitner, L. M. Bawa, J. Photochem. Photobiol. A. **305**, 67 (2015).

[19] Q. Xiao, O. Linli, Chem. Eng. J. **148**(2–3), 248 (2009).

[20] Z. Y. Li, M. S. Akhtar, O. B. Yang, J. Nanosci. Nanotechnol. **15**(9), 6675 (2015).

[21] V. O. Kollath, Q. Chen, R. Closset, J. Luyten, K. Traina, S. Mullens, A.R. Boccaccinic, R. Cloots, J. Eur. Ceram. Soc. **33**, 2715 (2013).

[22] L. Grinis, S. Dor, A. Ofir, A. Zanban, Photochem. Photobiol. A: Chem. **198**, 52 (2008).

[23] H. Chang, H.-T. Su, W.-A. Chen, K.D. Huang, S.-H. Chien, S.-L. Chen, C.-C. Chen, Sol. Energy. **84**, 130 (2010).

[24] A. U. Itodo, H. U. Itodo, M. K. Gafar, J. Appl. Sci. Environ. Manage. **14**(4), 141 (2010).

[25] T. S. Chandra, S. N. Mudliar, S. Vidyashankar, S. Mukherji, R. Sarada, K. Krishnamurthi, V. S. Chauhan, Bioresour. Technol. **184**, 395 (2015).

[26] K. Ullah, S. Ye, L. Zhu, Z.-D. Meng, S. Sarkar, W.-C. Oh, Mater. Sci. Eng., B. **180**, 20 (2014).

[27] L.-Y. Yang, S.-Y. Dong, J.-H. Sun, J.-L. Feng, Q.-H. Wu, S.-P. Sun, J. Hazard. Mater. **179**, 438 (2010).

_____
*Corresponding authors: kbussarin@gmail.com
                              mpanapoy@hotmail.com